Experimental investigation of a regime of Wigner ergodicity in microwave rough billiards

Y. Hlushchuk,[1] L. Sirko,[1] U. Kuhl,[2] M. Barth,[2] and H.-J. Stöckmann[2]
[1]*Institute of Physics, Polish Academy of Sciences, Al. Lotników 32/46, 02-668 Warszawa, Poland*
[2]*Fachbereich Physik, Philipps-Universität Marburg, Renthof 5, D-35032 Marburg, Germany*
(Received 16 October 2000; revised manuscript received 4 January 2001; published 27 March 2001)

We study experimentally a new regime of Wigner ergodicity [K.M. Frahm and D.L. Shepelyansky, Phys. Rev. Lett. **79**, 1833 (1997)] in a microwave rough billiard. We show that in the Wigner regime, eigenstates are extended over the whole energy surface but have a strongly peaked nonergodic structure. The Shannon width of the eigenstate distributions is calculated to estimate their spreads and to find their departure from the ergodic distributions.

DOI: 10.1103/PhysRevE.63.046208 PACS number(s): 05.45.Mt

In certain classes of chaotic billiards the quantum eigenstates are known to be localized in angular momentum space for the relatively low-level numbers [1–3]. This phenomenon can be observed in billiards being a small distortion of the circular billiard such as the stadium billiard [1] and weakly deformed (rough) circular billiards [2,3]. However, according to Shnirelman theorem [4] the eigenstates become ergodic for sufficiently high level numbers [5,6]. The question arises how does the transition from localized to ergodic regime occur? Analyzing rough circular billiards, Frahm and Shepelyansky [6] predicted theoretically that the transition from localized states to the ergodic ones could pass through the intermediate regime of Wigner ergodicity. In this regime the states are nonergodic but composed of rare strong peaks that are distributed on the whole energy surface. At the same time the nearest-neighbor level-spacing statistics is still given by the Wigner distribution.

In this paper we present the experimental investigation of the regime of Wigner ergodicity. In the experiment we used a brass cavity in the shape of a rough half circle (Fig. 1). The cavity sidewalls are made of three segments. The segments 1 and 2 are described by the radius function $R^i(\theta)=R_0+\Sigma_{m=2}^{M}a_m^i\sin(m\theta+\phi_m^i)$, where $i=1,2$, the mean radius $R_0=16.0$ cm, $M=20$, a_m^i and ϕ_m^i are uniformly distributed on $[0.076,0.084]$ cm and $[0,2\pi]$, respectively, and $0\leqslant\theta<\pi/2$. From many possible sets of the coefficients a_m^i and phases ϕ_m^i, we chose the ones that gave a smooth transition between the segments 1 and 2. We would like to note that we decided to use a rough (weakly deformed) half-circular cavity instead of a rough circular cavity because of the special properties of an undeformed half-circular billiard. A half-circular billiard is equivalent to the desymmetrized circular billiard with the odd symmetry with respect to the reflection at the diameter. In a circular billiard the eigenvalues with the angular momentum $l\neq 0$ are twofold degenerate. It means that in a weakly deformed circular cavity many of the low-level eigenvalues are nearly degenerate and they could not be possibly distinguished in the measurements. Using a weakly deformed half-circular cavity we overcame this serious problem.

The surface roughness of a billiard is characterized by the function $k(\theta)=(dR/d\theta)/R_0$. Thus for our billiard we have the angle average $\tilde{k}=[\langle k^2(\theta)\rangle_\theta]^{1/2}\simeq 0.183$. In such a billiard the dynamics is diffusive in orbital momentum due to collisions with the rough boundary because $\tilde{k}$ is above the chaos border $k_c=M^{-5/2}=0.000\,56$ [2]. The roughness parameter $\tilde{k}$ determines also other properties of the billiard [6]. The eigenstates of a rough half-circular billiard are localized for the level number $N<N_e=1/128\tilde{k}^4\simeq 7$. The dynamic localization in a rough microwave cavity was observed experimentally by Sirko *et al.* [3]. The border of Breit-Wigner regime is $N_W=M^2/48\tilde{k}^2\simeq 249$. It means that between $N_e<N<N_W$ Wigner ergodicity ought to be observed and for $N>N_W$ Shnirelman ergodicity should emerge.

One should mention that rough billiards and related systems are also of considerable interest elsewhere, for example, in the context of ballistic electron transport in microstructures [7], microdisc lasers [8,9], and localization in discontinuous quantum systems [10].

It is well known that the Helmholtz equation describing the electromagnetic field inside a thin microwave cavity [11] can be equivalent to the Schrödinger equation in a two-dimensional quantum billiard [12]. The equivalence takes place for frequencies below the onset of the three-dimensional (3D) electromagnetic mode at $f_{cut}=c/2h$, where h is the height of a cavity and c is the speed of light. In our experiment the cavity had the height $h=0.8$ cm and was excited at frequencies up to 10 GHz, thus much below the frequency $f_{cut}\simeq 18.7$ GHz.

In order to investigate the Wigner ergodicity, knowledge

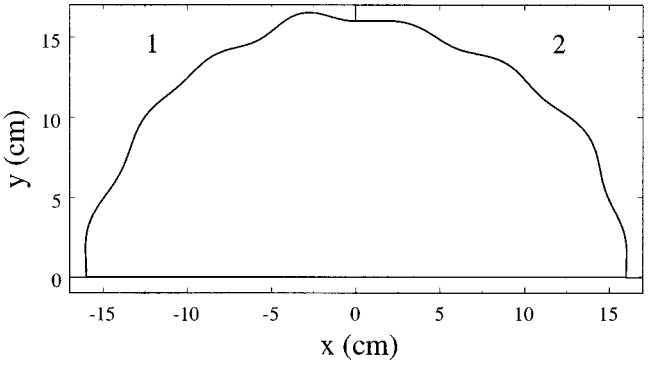

FIG. 1. Sketch of the rough half-circular microwave cavity in the xy plane. The dimensions are given in cm. The main segments of the cavity are marked 1 and 2 (see text).

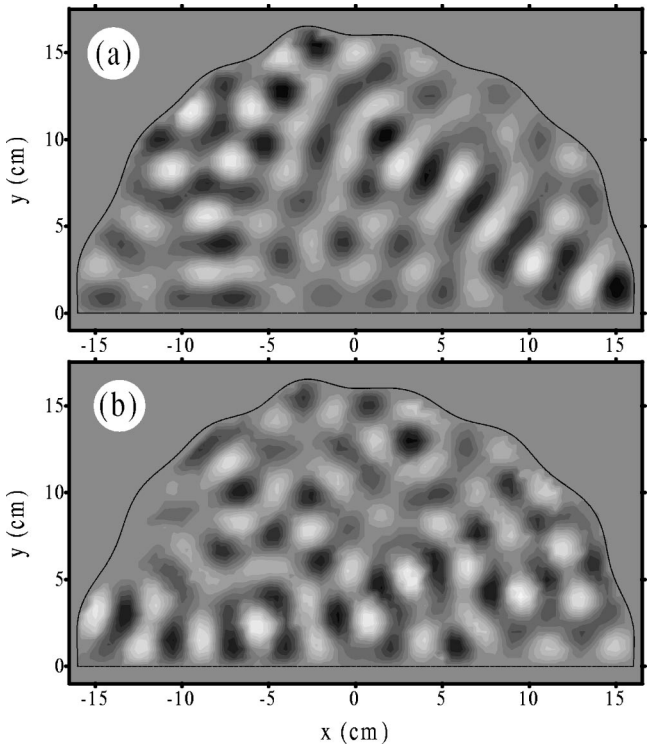

FIG. 2. Experimental eigenfunctions with the level numbers (a) $N=120$ ($f_N=9.72$ GHz), (b) $N=127$ ($f_N=9.98$ GHz). The amplitudes have been converted into a grey scale with white corresponding to large positive and black corresponding to large negative values, respectively.

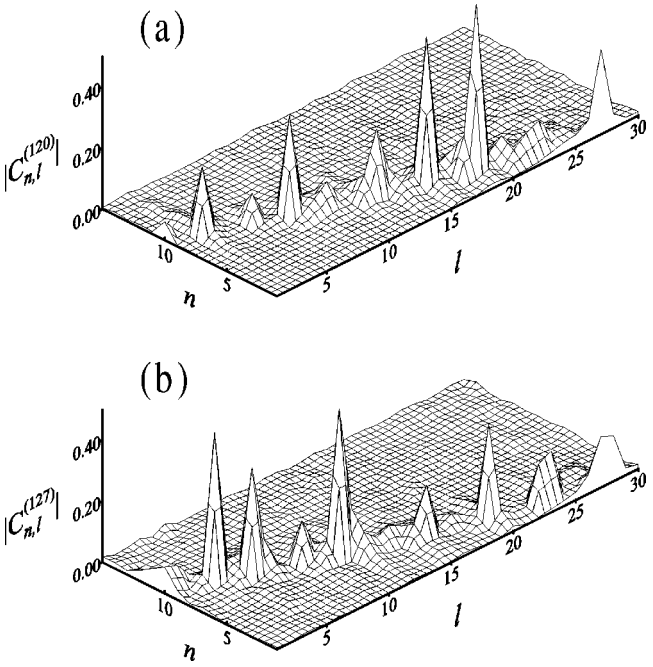

FIG. 3. Structure of the energy surface in the regime of Wigner ergodicity. Here we show the absolute amplitudes $|C_{nl}^{(N)}|$ for the eigenfunctions (a) $N=120$ and (b) $N=127$. The large peaks are distributed rarely but over the whole energy surface.

of the (electric field) eigenfunction is indispensable. To measure the eigenfunction we used the method described in [13]. It is based on the measurements of S matrix elements of the system. The matrix element S_{11} gave the quantity proportional to $|\Psi(x,y)|^2$ while the measurements of the transmission matrix elements S_{21} determined the sign of $\Psi(x,y)$. Using a vector network analyzer (Wiltron 360B), each eigenfunction was sampled with the step of 5 mm in both x and y directions leading to a total of about 1500 data points. In this way we were able to measure the eigenfunctions with the level numbers $N=4-127$. The range of corresponding eigenfrequencies f_N was from 2.07 GHz to 9.98 GHz. Despite of the semi-circular geometry of the cavity, the resonances $N=115$ and $N=116$ were not resolved within the experimental resolution, being approximately 8 MHz in the vicinity of 9.5 GHz. Fortunately, this cluster of two resonances was easily spotted out by the comparison of the experimental staircase function with the average number of levels predicted by the theoretical Weyl formula [14]. Better resolution of the resonances is possible in other experimental systems such as 3D resonating quartz blocks [15] and 2D superconducting cavities [16]. However, those systems are not so well suited as our cavity for the measurements of the eigenfunctions. The two examples of the measured eigenfunctions with the eigenvalues $E_N=k_N^2=(2\pi f_N/c)^2$, $f_N=9.72$ GHz and 9.98 GHz for the level number $N=120$ and $N=127$, respectively, are shown in Fig. 2. Both eigenfunctions, as it will be seen further, represent the case of Wigner ergodicity.

In order to reveal the structure of the energy surface we extracted experimental eigenfunction amplitudes $C_{nl}^{(N)}=\langle nl|N\rangle$ in the basis n,l of an unperturbed half-circular billiard, where $n=1,2,3,\ldots$ enumerates the zeros of the Bessel functions and $l=1,2,3,\ldots$ is the angular quantum number. The method of alternative extended Simpson's rule [17] was repeatedly used in 2D integration procedure. The uncertainty in evaluation of the amplitudes $|C_{nl}^{(N)}|$ is estimated to be 10%. The absolute amplitudes $|C_{nl}^{(N)}|$ are shown in Fig. 3. The eigenstates are extended over the energy surface but are composed of rare and strong peaks. The positions of the main peaks $|C_{nl}^{(N)}|\geqslant 0.2$ are marked by diamonds in Fig. 4. The error bars size is $2|C_{nl}^{(N)}|$. Figure 4 demonstrates that the largest peaks appear for those n and l that are close to the energy surface of a half-circular billiard $E_{nl}=(X_{l,n}/R_0)^2 \simeq E_N$, where $X_{l,n}$ is the nth zero of the Bessel function of order l. The empty circle marks the energy surface calculated from this formula under the assumption $|E_{nl}-E_N|/E_N \leqslant 0.02$. The full lines in Figs. 4(a) and 4(b) show the energy surface of a half-circular billiard estimated from the semiclassical formula [6] $\sqrt{l_{max}^2-l^2}-l\arctan(l^{-1}\sqrt{l_{max}^2-l^2}) + \pi/4=\pi n$, where $l_{max}^2=k_N^2R_0^2$. As we see the agreement between quantum and semiclassical results is excellent. The main peaks ($|C_{nl}^{(N)}|\geqslant 0.2$) are spread almost perfectly along the lines marking the energy surface of a half-circular billiard. The peaks are not equidistant but as it was predicted in [6] there are a lot of holes in their distribution.

Furthermore, we use the concept of the Shannon width [18] to estimate quantitatively the spread of the eigenstate

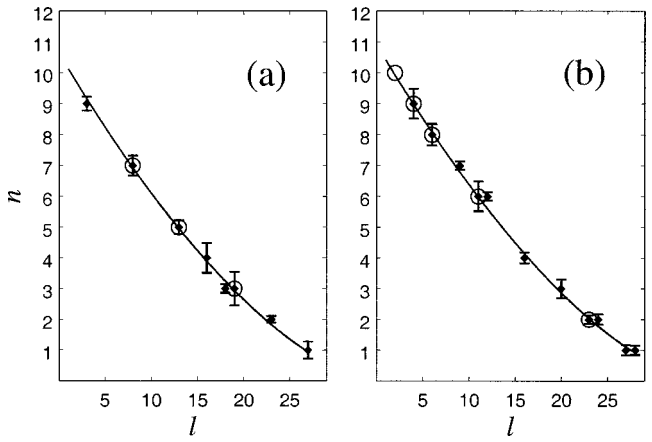

FIG. 4. Energy surface $H(n,l)=E_N$ for the eigenstates (a) $N=120$ and (b) $N=127$. The diamonds mark the main peaks of the eigenstates ($|C_{nl}^{(N)}|\geqslant 0.2$); the error-bars size is $2|C_{nl}^{(N)}|$; empty circles mark the energy surface for those n,l for which $|E_{nl}-E_N|/E_N\leqslant 0.02$. Full lines show the semiclassical estimation of the energy surface (see text).

distributions in the n,l basis. The Shannon width is defined as follows: $W^{(N)}=\exp(-\Sigma_{n,l}p_{nl}^{(N)}\ln p_{nl}^{(N)})$, where $p_{nl}^{(N)}=|C_{nl}^{(N)}|^2$. The basic properties of the width $W^{(N)}$ are the following: if a single state is occupied $W^{(N)}=1$; if the k states are equiprobably populated, $W^{(N)}=k$. The Shannon widths $W^{(N)}$ of the distributions presented in Figs. 3(a) and 3(b) are 11.7 and 14.6, respectively. Our preliminary numerical calculations [19] carried out for the billiard with the same mean radius $R_0=16.0$ cm but much larger roughness ($N_W\simeq 40$) show that for the states with the level number $N=120-127$, the width of the ergodic distributions is approximately $W^{(N)}\simeq 30$. It is important to note that the widths of the ergodic distributions are significantly larger than the ones measured in the regime of Wigner ergodicity.

Figure 5 shows the nearest-neighbor level-spacing distribution for the eigenstates $N=15-127$, thus within the predicted limits $N_e<N<N_W$ of Wigner ergodicity. The level-spacing statistics is very close to the Wigner distribution. The missing resonance only slightly modifies the counts in the first bin of the distribution. Together with the peaked structures of the eigenstates presented in Fig. 3, this is a further evidence that the eigenstates belong to a new regime of Wigner ergodicity.

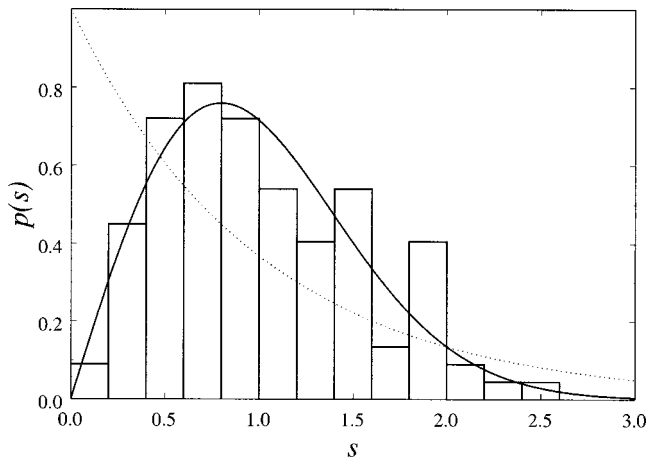

FIG. 5. Nearest-neighbor spacing distribution for the eigenstates $N=15-127$. The full line shows Wigner distribution. The dotted line marks Poisson distribution.

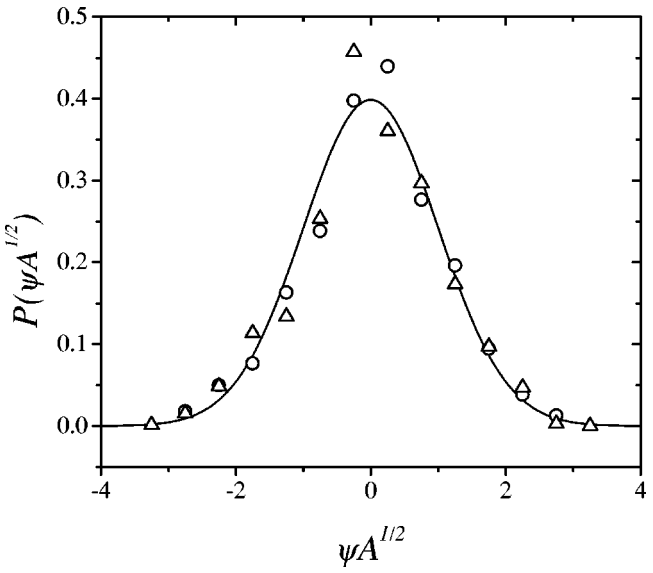

FIG. 6. Amplitude distribution $P(\psi A^{1/2})$ for the eigenstates $N=120$ (empty circles) and $N=127$ (empty triangles) constructed as histograms with bin equal to 0.5. The width of the experimental distribution $P(\psi)$ was rescaled to unity by multiplying the experimental, normalized to unity, eigenfunction by the factor $A^{1/2}$, where A denotes billiard's area. The full line shows standard normalized Gaussian prediction $P_0(\psi A^{1/2})=(1/\sqrt{2\pi})e^{-\psi^2 A/2}$.

An additional confirmation of ergodic behavior of the measured eigenfunctions can be also sought in the form of the amplitude distribution $P(\psi)$ [20,21]. For irregular, chaotic states the probability of finding the value ψ at any point inside the billiard, without knowledge of the surrounding values, should be distributed as a Gaussian, $P(\psi)\sim e^{-\beta\psi^2}$. The amplitude distributions $P(\psi)$ for the eigenfunctions $N=120$ and $N=127$ are shown in Fig. 6. They were constructed as normalized to unity histograms with the bin equal to 0.5. Each particular histogram was built using approximately 1500 values of an eigenfunction. The width of the experimental distribution $P(\psi)$ was rescaled to unity by multiplying the experimental, normalized to unity, eigenfunction by the factor $A^{1/2}$, where A denotes billiard's area (see formula (23) in [21]). The agreement with the standard normalized Gaussian prediction $P_0(\psi)=(1/\sqrt{2\pi})e^{-\psi^2/2}$ is quite good though there are some deviations in the vicinity of zero.

The amplitudes $C_{nl}^{(N)}$ determine the local density of states in the regime of Wigner ergodicity by

$$\rho_W(E-E_{nl})=\left\langle \sum_N \delta(E-E_N)|C_{nl}^{(N)}|^2 \right\rangle. \qquad (1)$$

The average is performed over a sufficiently large energy

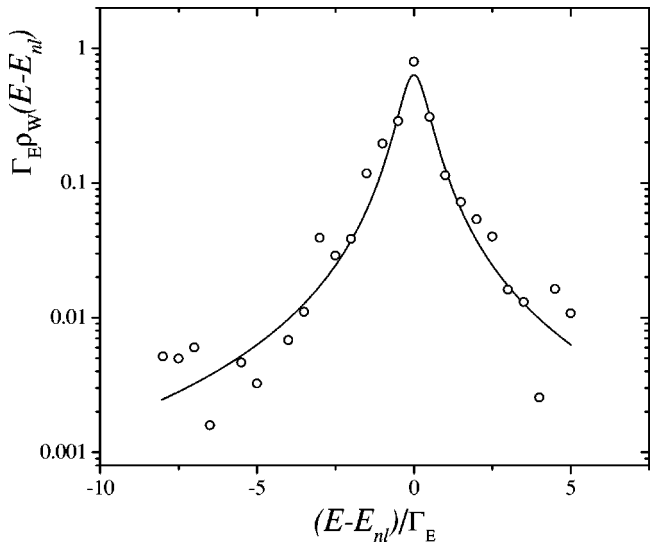

FIG. 7. Experimental local density of states ρ_W (empty circles) compared to theoretical Breit-Wigner distribution ρ_{BW} (full line). Ten experimental eigenstates with the level number N between 87 and 127 were used in calculation of ρ_W.

interval. Theoretically, the local density of states is given by the Breit-Wigner distribution [6],

$$\rho_{BW}(E-E_{nl})=\frac{1}{\pi}\frac{\Gamma_E/2}{(E-E_{nl})^2+\Gamma_E^2/4}. \tag{2}$$

The equation (2) is valid for $N<N_W$ and $\Delta E=E-E_{nl}<E_b$, where $E_b=2l_{max}^2/(R_0^2\sqrt{l_{max}^2-l^2})$. The width of the ρ_{BW} distribution is given by $\Gamma_E=2N\sqrt{l_{max}^2-l^2}/(N_W R_0^2)$.

The comparison of the experimental local density of states ρ_W and the Breit-Wigner distribution ρ_{BW} is shown in Fig. 7. The experimental points are the average of the results obtained from the ten eigenstates lying between $N=87-127$. All the chosen eigenstates were extended over the energy surface but displayed strong peaks and holes in their structure. The overall agreement of the experimental results for ρ_W with the theoretically predicted ρ_{BW} is very good. This additionally confirms that presented in this paper eigenstates lie in a new regime of Wigner ergodicity.

Summarizing, we measured experimentally the eigenfunctions of the rough half-circular billiard. We showed that for $N_e<N<N_W$ some of the eigenstates are extended over the energy surface of a half-circular billiard but have strongly peaked nonergodic structure. This observation was quantitatively confirmed by the calculation of the Shannon widths of the eigenstates distributions. Moreover, the nearest-neighbor level-spacing statistics was very close to the Wigner distribution, the amplitude distribution $P(\psi)$ was close to the Gaussian distribution, and finally the local density of states ρ_W was very close to the Breit-Wigner density ρ_{BW}. All these properties of the measured eigenstates confirm the existence of a new regime of Wigner ergodicity.

Y.H. and L.S. acknowledge partial support by KBN Grant No. 2 P03B 023 17. The Deutsche Forschungsgemeinschaft is thanked for financial support and for bearing the expenses of the two-week stay of Y.H. in Marburg. We thank Sz. Bauch for reading the manuscript and useful remarks.

[1] F. Borgonovi, G. Casati, and B. Li, Phys. Rev. Lett. **77**, 4744 (1996).
[2] K. Frahm and D. Shepelyansky, Phys. Rev. Lett. **78**, 1440 (1997).
[3] L. Sirko, Sz. Bauch, Y. Hlushchuk, P. M. Koch, R. Blümel, M. Barth, U. Kuhl, and H.-J. Stöckmann, Phys. Lett. A **266**, 331 (2000).
[4] A. Shnirelman, Usp. Mat. Nauk. **29**, 18 (1974).
[5] O. Bohigas, M. J. Giannoni, and C. Schmit, Phys. Rev. Lett. **52**, 1 (1984).
[6] K. Frahm and D. Shepelyansky, Phys. Rev. Lett. **79**, 1833 (1997).
[7] Ya. M. Blanter, A. D. Mirlin, and B. A. Muzykantskii, Phys. Rev. Lett. **80**, 4161 (1998).
[8] Y. Yamamoto and R.E. Sluster, Phys. Today **46** (6), 66 (1993).
[9] J. U. Nöckel and A. D. Stone, Nature **385**, 45 (1997).
[10] F. Borgonovi, Phys. Rev. Lett. **80**, 4653 (1998).
[11] J. D. Jackson, *Classical Electrodynamics* (Wiley, New York, 1975).
[12] H.-J. Stöckmann and J. Stein, Phys. Rev. Lett. **64**, 2215 (1990); H.-J. Stöckmann, *Quantum Chaos, an Introduction* (Cambridge University Press, Cambridge, 1999), Chap. 2.
[13] U. Kuhl, E. Persson, M. Barth, and H.-J. Stöckmann, Eur. Phys. J. B **17**, 253 (2000).
[14] M. C. Gutzwiller, *Chaos in Classical and Quantum Mechanics* (Springer-Verlag, New York, 1990), p. 259.
[15] C. Ellegaard, T. Guhr, K. Lindemann, J. Nygård, and M. Oxborrow, Phys. Rev. Lett. **77**, 4918 (1996).
[16] H. Alt, C. Dembowski, H.-D. Gräf, R. Hofferbert, H. Rehfeld, A. Richter, and C. Schmit, Phys. Rev. E **60**, 2851 (1999).
[17] W. H. Press, B. P. Flannery, S. A. Teukolsky, and W. T. Vetterling, *Numerical Recipes* (Cambridge University Press, Cambridge, 1987), Chap. 4.
[18] R. Blümel, A. Buchleitner, R. Graham, L. Sirko, U. Smilansky, and H. Walther, Phys. Rev. A **44**, 4521 (1991).
[19] Y. Hlushchuk, A. Błędowski, N. Savytskyy, and L. Sirko (unpublished).
[20] M. V. Berry, J. Phys. A **10**, 2083 (1977).
[21] S. W. McDonald and A. N. Kaufman, Phys. Rev. A **37**, 3067 (1988).